In presenting the dissertation as a partial fulfillment of the requirements for an advanced degree from the Georgia Institute of Technology, I agree that the Library of the Institute shall make it available for inspection and circulation in accordance with its regulations governing materials of this type. I agree that permission to copy from, or to publish from, this dissertation may be granted by the professor under whose direction it was written, or, in his absence, by the Dean of the Graduate Division when such copying or publication is solely for scholarly purposes and does not involve potential financial gain. It is understood that any copying from, or publication of, this dissertation which involves potential financial gain will not be allowed without written permission.

_____

7/25/68

ORDER STRENGTHENING IN EQUIATOMIC COPPER-GOLD

A THESIS

Presented to

The Faculty of the Graduate Division

by

E. Walton Horne

In Partial Fulfillment

of the Requirements for the Degree

Master of Science in Metallurgy

Georgia Institute of Technology

March 1969

ORDER STRENGTHENING IN

EQUIATOMIC COPPER-GOLD

Approved:

Date approved by Chairman: 2/27/69

ACKNOWLEDGMENTS

The author wishes to express his gratitude to Dr. E. A. Starke, Jr., for his help, encouragement and patience during the course of this work. The encouragement and understanding expressed by the author's parents, Mr. and Mrs. E. W. Horne, Jr., are deeply appreciated. The help and encouragement derived from the author's fiancée, Miss Marilyn Neal, during the course of the work, and especially in the typing of the rough draft, are acknowledged with special appreciation.

The author is also grateful to the National Institute of Dental Research for its financial support of this study.

TABLE OF CONTENTS

LIST OF TABLES

LIST OF FIGURES

SUMMARY

The strengthening induced on ordering a previously disordered sample of equiatomic Cu-Au at constant temperature was studied, using hardness measurements and high-angle x-ray diffraction.

It was found that a transient decrease in hardness occurs at a very early ordering stage. Concomitantly, the sample began to exhibit preferred orientation and an inflection in the growth rate of the ordered domains was observed. These effects can be explained in terms of a reversion mechanism in which those nuclei dissolve which have not attained a certain critical size or are not properly oriented.

Following the dip in hardness after short aging times, the strength of the alloy once again increased, reached a maximum value and then decreased. It is felt that the strength increase is due to coherency strains and tetragonal distortion strains. During the final hardness decrease the domain size began to increase rapidly. The final decrease is a result of twinning and loss of coherency between the ordered nuclei and the disordered matrix. The latter effect is felt to be the cause of the rapid growth of the ordered domains during the later stages of ordering.

CHAPTER I

INTRODUCTION

Order-Disorder Transformations

Order-disorder phenomena have been the subject of many investigations since the verification of such transformations. There are two general types of order possible in an alloy: short-range order and long-range order.

In an alloy possessing short-range order, the number of unlike atom pairs is greater than the composition would indicate. The short-range order parameter, σ, measures the extent to which, on the average, each atom is surrounded by unlike neighbors. Bethe[1] has defined the short-range order parameter as:

$$\sigma = (q - q_r)/(q_o - q_r)$$

where q = the fraction of nearest neighbor bonds between unlike atoms,

q_o = the fraction of nearest neighbor bonds between unlike atoms for complete order,

q_r = the fraction of nearest neighbor bonds between unlike atoms for random order.

For an AB alloy: $q_o = 1$, $q_r = 1/2$, and, therefore, $\sigma = 2q - 1$.

An alloy is said to possess long-range order if the atoms of a given species tend to occupy specific lattice sites, e.g., in Cu_3Au the

copper atoms occupy the corner positions in the fcc lattice, while the gold atoms are found at the face centers. The long-range order parameter is a measure of how completely A-atom sites are occupied by A-atoms, and B-atom sites are occupied by B-atoms in the lattice. The long-range order parameter, S, has been defined by Bragg and Williams:[2]

$$S = (p - 4)/(1 - r)$$

where p = the probability that an A-atom site is filled by an A-atom

r = fraction of total sites occupied by A-atoms for perfect order.

When ordering in an AB alloy, A-atoms in some nuclei may occupy superlattice positions occupied by B-atoms and other nuclei. When these nuclei grow and impinge on each other, the plane of contact is known as an antiphase domain boundary, the individual large ordered nuclei being known as antiphase domains. As annealing continues, some antiphase domains grow at the expense of others until each grain should enclose a single domain.

Two differing general mechanisms for disorder-to-order transformations have been proposed. One mechanism involves the homogeneous ordering of the alloy, beginning at all points in the crystal simultaneously. The other mechanism describes the ordering process in terms of the formation of stable, highly-ordered nuclei which grow at the expense of the disordered matrix. These two mechanisms will be discussed in greater detail in relation to the ordering of CuAu below.

The disorder-order transformation in an alloy may or may not

affect its crystal structure. Cu_3Au, for example, has the fcc structure in both the disordered and the ordered condition. (It should be noted, however, that the Bravais lattice of the alloy does change from face-centered cubic to four interpenetrating simple cubic lattices during the transformation.) In contrast, the alloy CuAu changes from fcc in the disordered condition to fct in the ordered state (below 375°C). While the lattice parameter change in Cu_3Au during ordering is roughly one part in a thousand, the c-axis in CuAu contracts about 5.3%, and the a-axes lengthen about 2.3% each.[3]

Order Strengthening

Since the transformation of an alloy from the disordered to the ordered state has such a great effect on its structure, it should naturally be expected that the mechanical properties of the system would also be changed. This is found to be the case for both short-range and long-range ordering.

Fisher[4] has proposed a mechanism for the strengthening of an alloy possessing short-range order. He points out that, in a crystal of a pure metal or in a completely random solid solution, the dislocations present are in a state of neutral equilibrium at zero stress. Any motion of the dislocation recreates perfect lattice or random matching of atoms across its glide plane. In a crystal with local order of the alloy components, the dislocation is in a state of stable equilibrium. Any motion would destroy the local order across the glide plane, forming a more random structure of higher energy. Thus, the dislocation can move only under the action of a definite stress. The stress increment that is required to just maintain the displacement of

such a dislocation (in the absence of diffusion) is a measure of the strengthening effect. Similar strengthening is not always found in long-range order, since dislocations may move in pairs called superdislocations, the second dislocation repairing the disorder introduced by the first. In this way perfect order is left across the glide plane.

Strengthening is also found in long-range ordering alloys at certain stages in the ordering process. It is necessary to consider the cases in which there is no change in crystal structure on ordering separately from those involving a crystal structure change.

For the comparatively larger group of alloys which undergo no crystal structure change on ordering, the important variables in order hardening seem to be incomplete order, antiphase domain boundaries, and paired dislocations.[5] Many theories have been advanced to explain strengthening in these alloys. Two different aspects of the strengthening in such alloys must be considered: the flow stress maximum observed when flow stress is determined as a function of annealing time, and the effect of ordering on the work hardening rate. Several of the more prominent theories for each of these effects are presented below.

To account for the flow stress maximum, Marcinkowski and Miller[6] visualize the partially ordered specimen as being short-range ordered with highly ordered domains. The short-range order causes a drag on moving dislocations by the Fisher mechanism (described above). The flow stress maximum is regarded as being due to a balance between the drag due to short-range order, which decreases as the long-range order parameter, S, increases, and increased cross-slip as S increases. This increased cross-slip causes the short-range order to be destroyed more

rapidly, thus raising the flow stress. (Cahn,[5] on the basis of optical micrography, has questioned the assumption of increased cross-slip with increasing order.)

Stoloff and Davies[7] propose that superdislocations disappear entirely at S = 0.2. Below that value, slip proceeds by single dislocations which create many wrong bonds as they move through the crystal. Therefore, these single dislocations move at a fairly high stress. As S increases, single dislocations associate into superdislocations, fewer wrong bonds are formed, and the flow stress decreases.

Cahn[5] has advanced the following mechanism for the flow stress maximum (based on a mathematical model by Gehlen and Cohen[8]). He suggests that there are many microdomains, containing about five atoms each, suspended in the volume of ordered matrix (about $10^{21}/cm^3$). Hardening occurs in a similar way to that found due to Guinier-Preston zones in a precipitation hardening alloy. Passage of dislocations, even superdislocations, through these microdomains shears them, increasing their periphery and, therefore, the number of wrong bonds. This requires energy, and thus the alloy is stronger.

Flinn[9] has suggested that the principal obstacle to slip in ordered alloys at temperatures too low for rapid diffusion is the effect of antiphase domain boundaries. Whenever a superdislocation passes through an antiphase domain boundary, additional new boundary is formed, adding extra energy.

Kear[10] attributed the steep work hardening rate in Cu_3Au to pinning of expanding dislocation loops by segments which cross-slip onto (100) planes. Stoloff and Davies[11] propose a similar model. They

reason that there is a finite probability that screw components will cross-slip onto another {111} plane. If cross-slip occurs a strong barrier will be created, and moving either of the unit dislocations comprising the barrier would create additional antiphase boundary. Thus the unit dislocations are effectively sessile. This will prevent additional dislocations from being produced by the same source. New sources are required to operate, and eventually most of the dislocation sources will be exhausted.

Vidoz and Brown[12] attribute work hardening in ordered alloys to superjogs formed when superdislocations cut forest dislocations present in the crystal. Work hardening results from an increase in the superjog density combined with the production of a trailing tube of antiphase domain boundary as the superdislocation continues to move. The production of antiphase domain boundary requires energy, and thus work hardening results.

Flinn[9] points out that deformation of a polycrystalline material requires slip on intersecting slip planes to relieve stress concentrations at grain boundaries. In an ordered material this type of slip results in a high work hardening rate, since the domain size is rapidly reduced as the slipped planes become new antiphase boundaries.

It can be seen from the large number of conflicting theories concerning order strengthening that the subject is not yet well understood. There remains much work to be done in order to conclusively state the mechanism for this phenomenon in alloys which do not undergo a crystal structure change on ordering. Far less work has been done related to the mechanical properties of ordered alloys which undergo a

crystal structure change on ordering. The increase in hardness on ordering is usually attributed to internal strains generated by the change in crystal structure. The more prominent theories describing ordering in these alloys will be discussed below in connection with the proposed hardening mechanisms for CuAu.

Ordering in CuAu

Kurnakov et al.[13] has predicted the "compounds" Cu_3Au and CuAu from physical and mechanical properties prior to the x-ray work by Johansson and Linde.[14] The alloy CuAu possesses the fcc crystal structure in the disordered state above about 410°C. At lower temperatures the equilibrium state is complicated by the existence of two crystallographic structures in the ordered state. Below about 380°C the structure is face-centered tetragonal with alternate (002) planes composed of all gold or all copper atoms, and c/a = 0.92. This fct superlattice is known as CuAu I. The superlattice formed between 380°C and 410°C may be described by an orthorhombic modification of the CuAu I structure, in which the gold and copper atoms change layers along the a- or b-axis every fifth cell. It is known as CuAu II. The CuAu I and CuAu II structures are shown in Figure 1.

CuAu I has the most common superlattice of those alloys which undergo a crystal structure change on ordering the $L1_0$ superlattice. Other alloys possessing this lattice type include CoPt, FePt, and FePd.

Two basic theories have been advanced to explain the kinetics of the disorder-order transformation in CuAu. The most revealing early work was that due to Borelius.[15] Based on thermodynamic considerations, he described the transformation as a homogeneous ordering process at

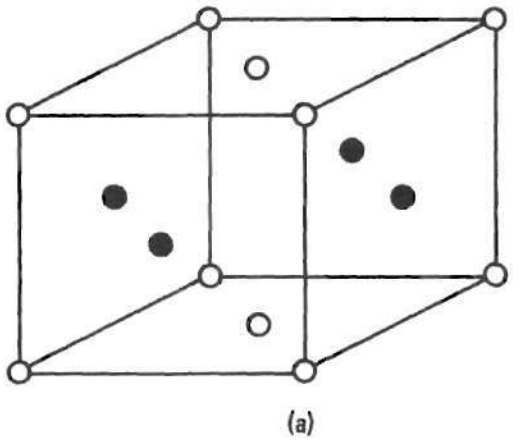

(a)

○ Cu

● Au

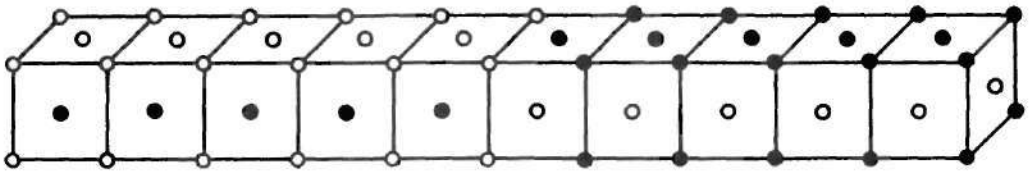

(b)

Figure 1. Ordered Structures in CuAu: (a) CuAu I (below 380°C), (b) CuAu II (380° - 410°C).

low temperatures (200° to 300°C). Between 330° and 440°C ordering was suggested to occur by a nucleation and growth process.

Harker[16] had proposed a similar model. He concluded that the order-disorder reaction in CuAu was not a phase change (nucleation and growth process) since the x-ray diffraction patterns obtained during the ordering process implied that the crystal structure changed gradually as aging continued. He defined an order-disorder transformation as "a process whereby one structure changes to another without the presence of sharp boundaries anywhere in the system at any time." Using Cu_3Au as an example, Harker envisioned the disorder to order transformation as beginning at completely ordered nuclei surrounded by regions of decreasing order as one proceeds away from the ordered nucleus.

Based on electrical resistivity measurements, Kuczynski, Hochman, and Doyama[17] suggested that the mechanism of ordering in CuAu is nucleation and growth at all temperatures. They found that a definite induction period for the inception of order exists, that the ordering rate is strongly dependent on the disordering temperature from which the sample is quenched, and that the ordering rate is also dependent on the ordering temperature.

Barker,[18] based on the work of Bethe[1] and Bragg and Williams,[2] described a model for the ordering of an alloy by nucleation and growth. This model is basically similar to those proposed by other investigators. The model is presented below with some of the experimental results of other investigators.

According to Barker's model, at high temperatures small regions of partial order will constantly be forming and dissolving in an

otherwise disordered alloy. Roberts[19] inferred a microlayering of copper and gold atoms above the critical temperature for ordering (T_c) from shift in diffuse x-ray peaks. Sato et al.[20] found short chains of antiphase domains scattered in the disordered lattice above T_c. Using high temperature electron diffraction it was found that these domains have a tendency to form a very degenerate CuAu II structure.

As cooling occurs, this short-range order becomes more extensive until the critical temperature is reached. Below this temperature, the nuclei are stable and grow into domains by absorbing each other and surrounding disordered material. (A model of ordering for Cu_3Au presented by Plalerink[21] includes the dissolution of nuclei with sub-critical size at this point.) Harker[16] suggested that the internal stresses generated by the crystal structure change on ordering in CuAu would be minimized if the nuclei formed as platelets along the {111} planes of the disordered matrix. The platelets were assumed to be so oriented that the c-axes of the fct cells, comprising a given platelet, lay along one of the original disordered cube axes X, Y, or Z. Harker reasoned that the internal stress would be minimized if the c-axes of adjacent platelets alternated in the sequence XYZXYZ . . . Hirabayashi and Weissmann,[22] using electron microscopy, and Hirabayashi and Ogawa,[23] using x-ray diffraction, found that the platelets form coherently with the disordered matrix along the $(110)_{cubic}$ planes, not (111) as predicted by Harker. This is due to the fact that strain is minimized if the $(101)_{tetr.}$ plane of the ordered phase becomes the conjugate plane of the $(110)_{cubic}$ plane of the disordered phase. Hirabayashi and Weissmann also found that the actual sequence of the c-axes of adjacent platelets is XYXYXY . . . , instead of XYZXYZ . . . as proposed by Harker.

Several investigators have reported the appearance of twins in CuAu specimens during ordering heat treatments.[3,17,22] The two types of twinning observed are described by Hirabayashi and Weissman.[22] They detected "microtwinning at an early ordering stage (after aging for two hours at 250°C) relieving the short range strains created by ordering; and formation of coarse twin lamellae varying in size from 1 - 3μ, which takes place at a more advanced ordering stage and results from the accommodations of long range strains set up by the growth of ordered lattice domains whose nucleation centers had different c-axis orientations." Kuczynski et al.[18] found that finer twin plates result from an increase in disordering temperature or a decrease in ordering temperature. Arunachalam and Cahn,[3] however, suggest that the structure assumed to be microtwins may actually be due to accidents of growth rather than mechanical twinning.

X-ray diffraction has been employed in the verification of the ordering mechanism in CuAu. Harker and Borelius advanced theories of homogeneous ordering in CuAu based on the fact that the lines of Debye-Scherrer x-ray photographs appeared to gradually shift and split to form the pattern characteristic of the ordered tetragonal structure. Harker[16] points out that in alloys which undergo phase changes the x-ray pattern at intermediate stages during the transformation contains lines characteristic of both structures. Since he did not observe such patterns for CuAu, he concluded that the order-disorder transformation in this alloy preceeded homogeneously. More recent x-ray measurements by Hirabayashi and Ogawa[23] and by O'Brien and Kuczynski[24] have revealed the ordered tetragonal pattern coexistent with the disordered face-

centered cubic lines. O'Brien and Kuczynski suggest that broadening of the x-ray peaks due to the internal strain in the lattice prevented the earlier investigators from resolving the two patterns.

As mentioned above, relatively little work has been done in the area of mechanical properties of CuAu and similar alloys. Nowack[25] was one of the first to investigate the relation between mechanical properties ordering variables of annealing time and temperature. His results are presented in Figure 2.

Harker[16] reported a general increase in the hardness of CuAu during the ordering heat treatment. The increase in hardness ran parallel with changes in the microstructure and x-ray diffraction pattern. It was suggested that the observed hardening was due to internal stresses caused by the coherent growth of the tetragonal ordered domains combined with interference to slip effected by irregularities in the slip planes of the ordered structure.

Nowack's[25] mechanical property measurements have been discussed by several investigators in relation to their own experiments. Hirabayashi and Weissmann[22] explained the peak hardness in Nowack's curves occurred at the ordering stage where the nuclei platelets are parallel to $(110)_{cubic}$ in the disordered matrix and exert coherency strains. It was felt that the decrease in hardness coincides with the onset of microtwinning. The hardness decay was explained to correspond to increased ordering after removal of coherency strains.

Hirabayashi and Ogawa[23] felt that the initial hardening was due entirely to coherency strains, and did not depend on short-range order strengthening (Fisher mechanism) or layering of the ordered and disordered

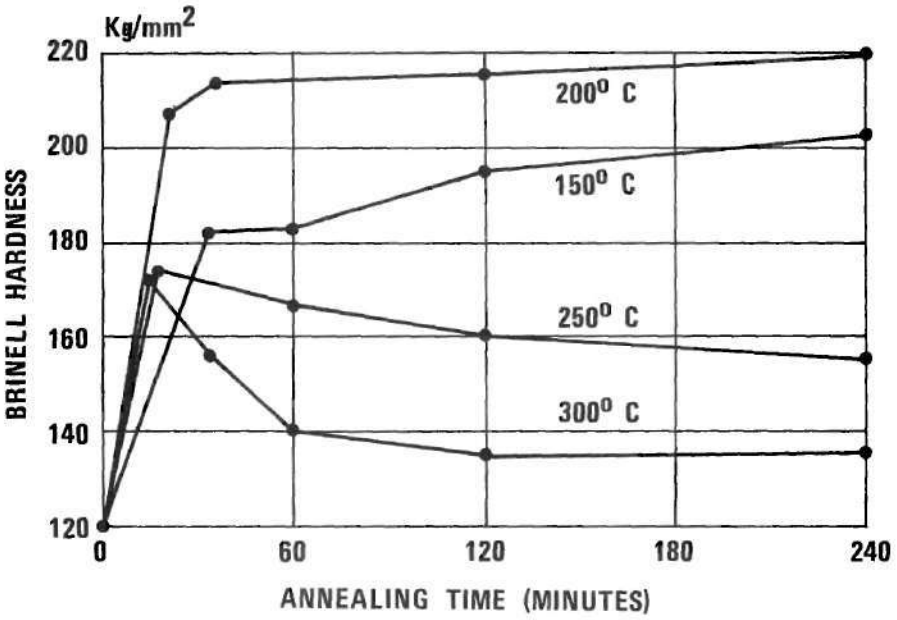

Figure 2. Age-Hardening Curves for CuAu Alloy.

structures as proposed by Harker.[16] As ordering proceeds, stresses were explained to be relieved by twinning, Harker's layered structure, self-deformation, and recrystallization.

In reviewing the recent work on mechanical properties of alloys which change crystal structure on ordering, Cahn[5] and Stoloff and Davies[26] cite the internal strains generated by this change as the major strengthening factor.

The most revealing study of the mechanical properties of CuAu to date is that due to Arunachalam and Cahn.[3] These investigators studied the change in hardness and flow stress of quenched and of cold worked disordered specimens as a function of annealing time and temperature. Optical and electron microscopy were also employed in the study.

The studies revealed an increase in hardness, then a softening for quenched disordered specimens ordered at 240° and 350°C. The softening effect was not observed in samples ordered at 150°C.

It was found that the increase in hardness for quenched, then ordered, alloys was greater than for cold worked then ordered alloys. It is noteworthy that the opposite is true for alloys which undergo no change in crystal structure on ordering. Another result of the investigation strengthens the theory that order has a greater effect on work hardening rate than on yield stress. The increase in yield stress on ordering was found to be less than the increase in hardness. Since large deformations are introduced during hardness measurements, the hardness of a metal should be dependent on the work hardening rate.

Arunachalam and Cahn discussed several factors contributing to order hardening in CuAu. It was pointed out that ordered CuAu I can

have both superlattice dislocations and single dislocations. Dislocations having Burgers vector $\frac{1}{2}\langle 110\rangle$ can move singly as they do not destroy order, while $\frac{1}{2}\langle 101\rangle$ and $\frac{1}{2}\langle 011\rangle$ dislocations must move in pairs. Thus, dislocations must change character when going from the disordered matrix into the ordered nuclei.

An additional strengthening effect is derived from the fact that a sessile interface dislocation is formed at the boundary due to the change in Burgers vector when a dislocation moves from a disorderd region into an ordered nucleus with different lattice spacing (Fleischer's model[27]). Such interface dislocations would present a barrier to succeeding dislocations. Fleischer's model is further complicated by the fact that jogs are formed at the order-disorder interface. These jogs cause even more difficulty for slip. Mechanisms proposed by Arunachalam and Cahn for the relief of internal stresses within the alloy included twinning, recrystallization in polycrystalline samples, and grain boundary migration.

Many questions remain unanswered concerning the mechanical properties of CuAu. It would be very desirable to know the relation between hardness and ordered domain size, degree of order, and internal lattice strains. Since the kinetics of the disorder-order transformation in CuAu are so highly dependent on the thermal and mechanical history of the sample, any study of the above relations should be designed such that the hardness measurements and the x-ray data are obtained from the same sample (as was done by Stoloff and Davies for Cu_3Au[28]). Such was the purpose and the method for the present investigation.

CHAPTER II

EXPERIMENTAL METHODS

Preparation of Sample

Melting

The bulk sample used throughout this investigation was prepared using high purity copper and gold. The materials were encapsulated in vycor tubing under 10^{-5} mm pressure after purging the system with argon. Melting was carried out in a high frequency induction furnace.

Homogenization

After cooling, the surface of the small cylinder obtained in the melting step was cleaned. First the surface layer was removed by swabbing for two minutes in a solution consisting of five volumes of glacial acetic acid, one volume of ortho-phosphoric acid, one volume of hydrochloric acid, and three volumes of nitric acid. After rinsing with water, the sample was placed in a reagent consisting of equal volumes of solutions containing 20 g. of KCN in 100 ml. of distilled water, and 20 g. of $(NH_4)_2S_2O_8$ in 100 ml. of distilled water, respectively.

After rinsing and drying the sample was encapsulated in vycor following the same procedure as for melting. The sample was placed in a Lindberg Hevi-Duty resistance furnace and maintained at 900°C for one week. After the homogenization treatment, the sample was quenched in ice water. A small portion of the sample was removed and analyzed by

Mac Millan Laboratories, Atlanta, Georgia. The composition was found to be 49.94 atomic per cent gold, 49.91 atomic per cent copper.

Mechanical Treatment

The sample was rolled at room temperature using a two-high laboratory rolling mill with 2.72 inch diameter rolls. Alternate rolling and recrystallization treatments were used to secure randomly oriented, fine-grained samples. The recrystallization treatments were conducted under vacuum at 500°C for twenty minutes and followed by ice water quenching.

A final sample size of 0.275 inch thickness by approximately 15/16 inch width by 1-1/2 inches length was obtained.

Disordering Heat Treatment

One surface of the sample was ground and polished flat. The sample was encapsulated in pyrex under vacuum, disordered for 5-1/2 hours at 450°C, and quenched in ice water. After quenching, and between ordering treatments, the sample was stored on dry ice to prevent structural alterations during storing periods.

Experimental Measurements

Aging Heat Treatment

Aging was effected by immersing the sample, held in a wire basket, in a Neslab Type T. 9/250 constant temperature bath, shown in Figure 3. The aging medium was Mobil high flash point oil maintained at 200°C±1°C.

Upon completion of the desired aging interval the sample was quenched in ice water. The oil was removed from the surface by rinsing twice in carbon tetrachloride. The surface was cleaned by placing the sample in a reagent consisting of equal volumes of solutions containing

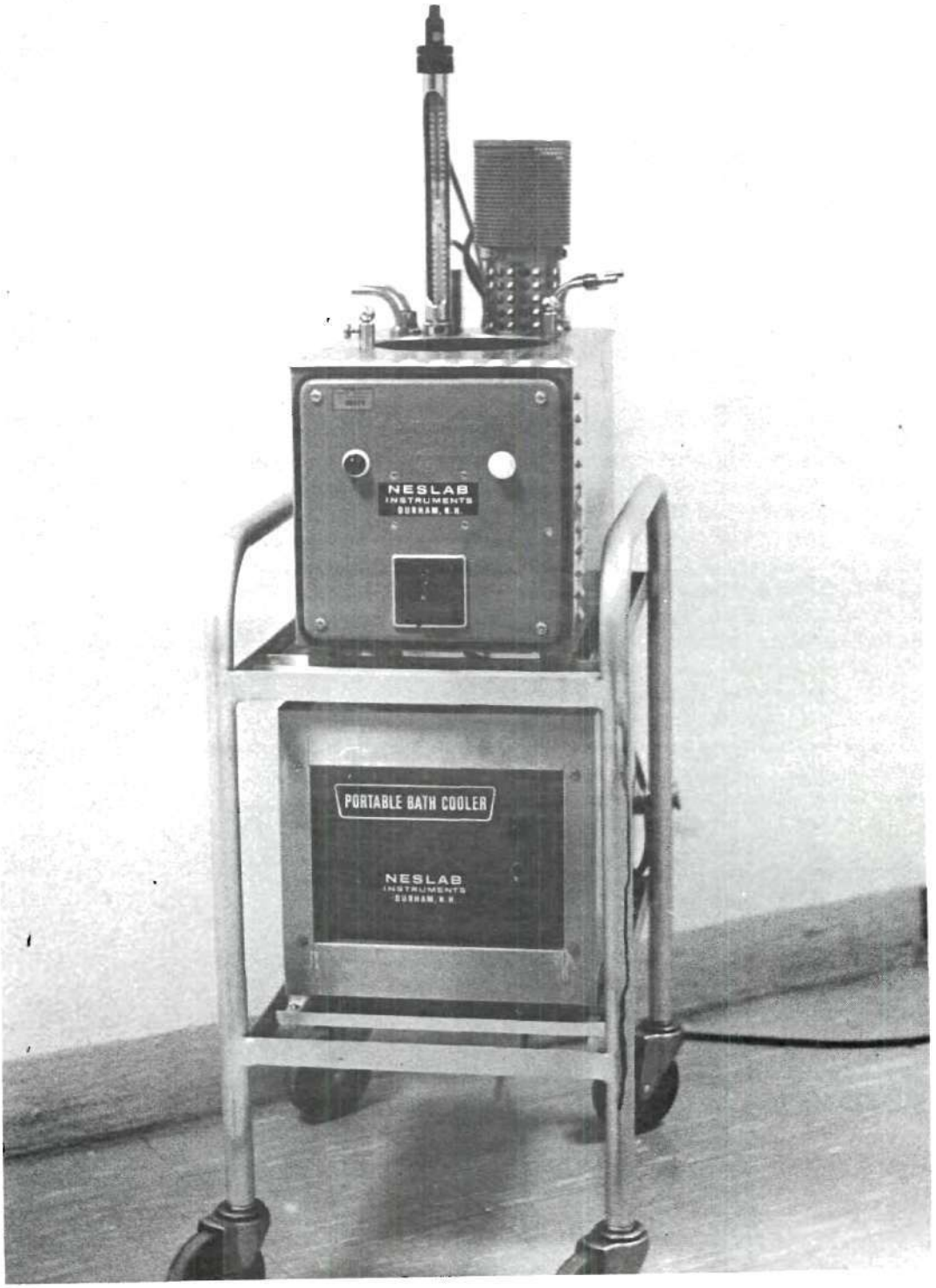

Figure 3. Constant Temperature Bath.

20 g. of KCN in 100 ml. of distilled water and 20 g. of $(NH_4)_2S_2O_8$ in 100 ml. of distilled water, respectively, for five minutes.

Metallography

One small portion of the bulk sample was removed after aging 140 hours at 200°C. The sample was mounted in "Quickmount" self-setting resin. The surface was ground flat, polished through 240, 320, 400, and 600 grit silicon carbide papers, lapped with 0.3 micron alumina compound. Lapping was followed by a final polish using the Vibra-Met and dilute 0.1 micron alumina compound suspended in distilled water. The sample was etched with aqua regia.

After photographing, the sample was removed from the mounting, encapsulated under vacuum in pyrex, and disordered at 450°C for 4-1/2 hours. The mounting and polishing procedure was repeated. The sample was etched in aqua regia. The photomicrographs are shown in Figure 4a and b.

Hardness Measurements

Hardness was determined after each aging treatment using a Vickers Pyramid Hardness Testing Machine equipped with a sliding table. A 20 Kg. load was used throughout the experiment. A minimum of three indentations were made for each aging treatment. The ocular reading was recorded as the average of the two diagonals of each indentation. Indentations for a given aging treatment were made at widely spaced points on the sample to insure a representative average.

After 27 minutes accumulated aging time the number of indentations was so great as to interfere with further measurements. These indentations were removed by grinding the surface using a Struers wet grinder

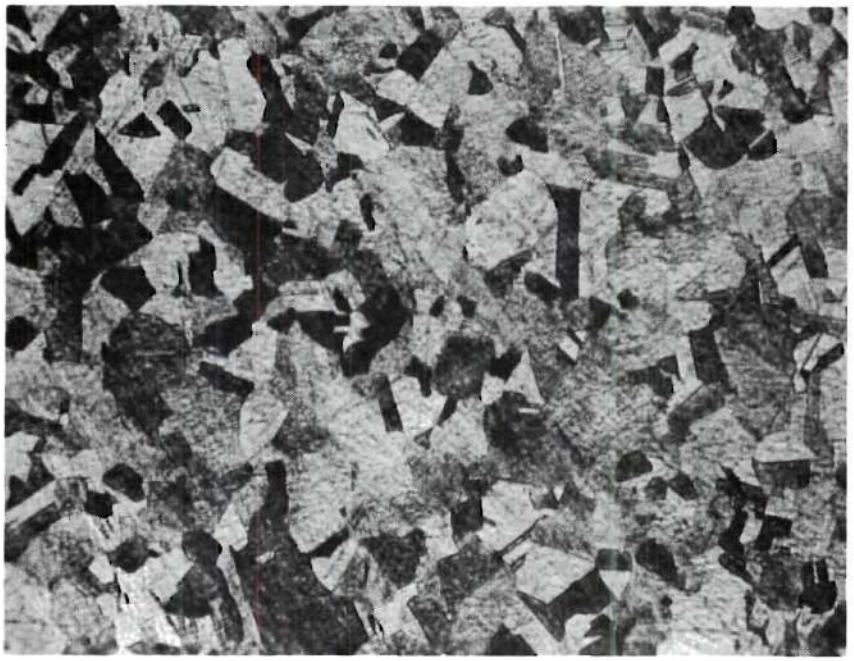

(A)

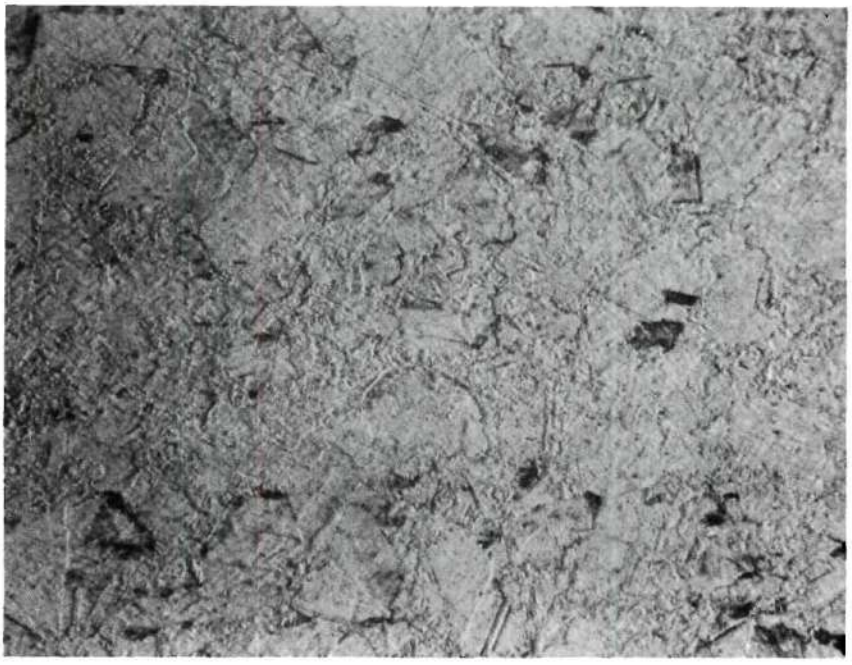

(B)

Figure 4. Photomicrographs of CuAu: (a) Disordered, (b) Ordered at 200°C for 140 Hours.

with silicon carbide papers of 240, 320, 400, and 600 grit successively. The surface was then lapped with 0.5μ chromium oxide compound. Comparison of hardness measurements made immediately before and after grinding indicated no change in hardness due to the grinding and polishing procedure.

X-ray Diffraction

Equipment. X-ray diffraction measurements were made using a General Electric XRD-6 diffractometer. The equipment employed a Warren doubly-bent LiF monochromator,[29] nickel filter in the primary beam, and pulse height discrimination in conjunction with a proportional counter. CuK_{α} radiation at 35 kV and 20 mA was used. The baseline voltage was 1.8 volts and the window was 2.0 volts. A 0.2° receiving slit was used in all cases. Air scattering was eliminated by evacuating the column around the specimen. The experimental arrangement is shown in Figure 5.

The diffracted intensity data taken was on a General Electric strip chart recorder. The rate meter response was 0.5 seconds in all cases.

Procedure. Quick scans were made when any significant change in hardness was noted or after a maximum of five minutes accumulated aging time since the previous scan. Scanning speed for the diffractometer was 2° 2θ per minute, recording chart speed was two inches per minute, and the scale factor was 100 counts per second.

When significant changes in the quick scan x-ray patterns were noted, detailed measurements were made. A diffractometer scanning speed of 0.2° 2θ per minute was employed with a recorder speed of two inches per minute. The chart scale was then ten inches per degree in 2θ.

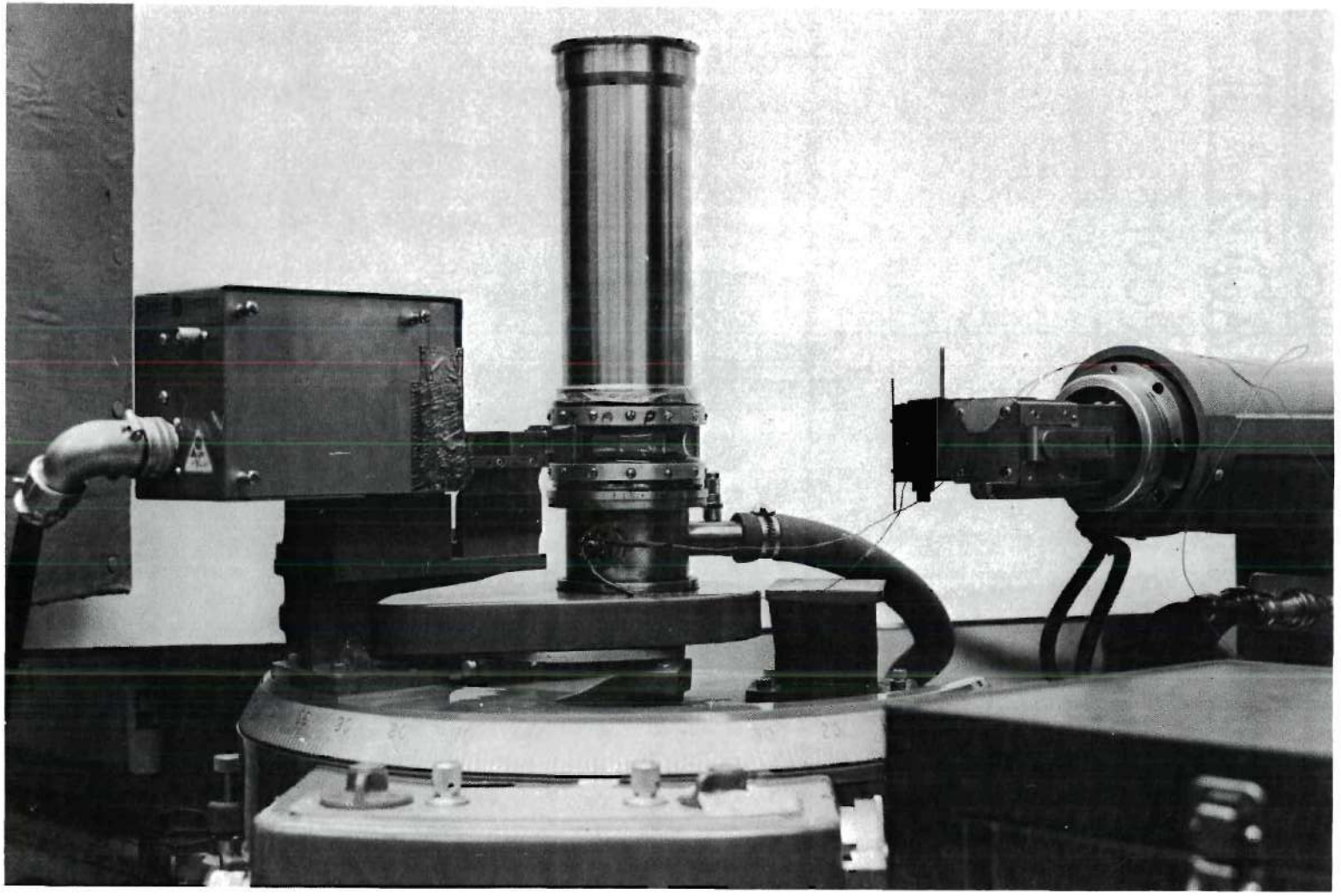

Figure 5. X-ray Diffractometer.

Scale factors were chosen so as to reveal the most possible detail. Depending upon the area scanned, scale factors of 50, 100, 200, 500, 1,000, or 5,000 counts per second were used.

Analysis of X-ray Data

Average Ordered Domain Size

The average ordered domain size was determined using the Scherrer equation[30] employing the method described by Stoloff and Davies[28] for removal of instrumental and strain broadening. The final form of the equation was:

$$t_D = \frac{0.9\lambda}{\beta \cos \theta_S}$$

where t_D is the average ordered domain size, λ is the x-ray wavelength (1.542A for CuK_α radiation), $\beta = \sqrt{B^2 - (B^*_{111})^2}$, B^*_{111} is the corrected breadth of the (111) peak at one half maximum intensity in the as quenched condition, B is the breadth of the given superlattice peak at one half maximum intensity, θ_S is the observed Bragg angle of the superlattice peak.

The value of B^*_{111} was determined in the following way. The average particle size of the sample was determined using Scherrer's equation:

$$t = \frac{0.9\lambda}{B_{111} \cos \theta_{111}}$$

where t is the average particle size, B_{111} is the observed breadth of the (111) peak at one half maximum intensity in the as quenched condition,

θ_{111} is the observed Bragg angle of the (111) peak in the as quenched condition.

The corrected value, B^*_{111}, was determined using Scherrer's equation as follows:

$$B^*_{111} = \frac{0.9\lambda}{t \cos \theta_S}$$

where the terms have the definitions described above.

An example of the calculation of ordered domain size is shown in Appendix A.

Bragg-Williams Long-Range-Order Parameter

The Bragg-Williams LRO parameter, S, was determined in two ways. First, an analysis analogous to that employed by Starke, Ogle, and Sparks[31] for Cu_3Au was used. The (110) and (110) superlattice peaks were compared with the (200) and the (220) fundamental peaks, respectively, using the following equation:

$$S^2 = \frac{A_S\left[f_{Cu} \exp(-M_{Cu}) + f_{Au} \exp(-M_{Au})\right]^2 \sin \theta_2 \sin 2\theta_S (1 + \cos^2 2\theta_m \cos^2 2\theta_f)}{A_f\left[f_{Cu} \exp(-M_{Cu}) - f_{Au} \exp(-M_{Au})\right]^2 \sin \theta_f \sin 2\theta_f (1 + \cos^2 2\theta_m \cos^2 2\theta_S)}$$

where A_S and A_f are the experimentally determined integrated intensities from the superlattice and fundamental reflections, respectively, $2\theta_m$ denotes the Bragg angle for the monochromator crystal, and the other terms have their usual meanings. The Debye-Waller factors, exp(-M), for copper and gold were taken from the work of Chipman[32] on Cu_3Au.

Due to the presence of preferred orientation in the sample, the above method did not yield consistent results between the two pairs of

peaks. The method described by LeFevre and Starke[33] in their work on Au_4V was employed in order to correct for the texture. This method, as it applies to the present study, is briefly described below.

The experimental integrated intensity of the ith peak of the superlattice spectrum may be written as:

$$E_i^0 = K\, R_i^0\, S^2\, T_i^0 \qquad (1)$$

where K is a constant independent of θ, S is the LRO parameter, and T_i^0 is the texture coefficient taking into account preferred orientation.[34] R_i^0 includes those terms which depend on the indices of the peak or its diffraction angle and is given by:

$$R_i^0 = m\left[f_{Cu}\, \exp(-M_{Cu}) - f_{Au}\, \exp(-M_{Au})\right]^2 LP \qquad (2)$$

where m is the multiplicity factor, f is the atomic scattering factor, exp(-M) is the temperature factor, L is the Lorentz factor and P is the polarization factor.

A similar expression may be written for the intensity of the jth peak of a fundamental spectrum:

$$E_j^f = K\, R_j^f\, T_j^f \qquad (3)$$

where the various terms have a similar meaning. It is not necessary to include a volume fraction term in the expressions (1) and (3) since it is the average degree of order which is of interest.

Since all of the superlattice peaks are resolved and measurable, we can write:

$$A = \frac{1}{I} \sum_{i=1}^{I} E_i^0/R_i^0 = \left\langle K\ S^2\ T_i^0 \right\rangle \qquad (4)$$

and

$$B = \frac{1}{J} \sum_{j=1}^{J} E_j^f/R_j^f = \left\langle K\ T_j^f \right\rangle \qquad (5)$$

from which we get:

$$A/B = \frac{K\ S^2 \left\langle T_i^0 \right\rangle}{K \left\langle T_j^f \right\rangle} = S^2 \frac{\left\langle T_i^0 \right\rangle}{\left\langle T_j^f \right\rangle} \qquad (6)$$

Since the ideal value of $\left\langle T_i^0 \right\rangle$ and $\left\langle T_j^f \right\rangle$ is one when many reflections are used for the average,[34] we can write:

$$S^2 = A/B$$

The experimental values of E_i^0 and E_j^f were determined in one of two ways. Peaks which were comparatively sharp and which covered a relatively small area were integrated using a K & E Planimeter, model 65 0000. Peaks which covered a larger area were integrated by tracing the outline of the peak onto recorder paper, cutting out the peak shape, weighing, and comparing the weight with that of a known area of the same paper.

A sample calculation of S is shown in the Appendix.

CHAPTER III

RESULTS

Strengthening in an equiatomic CuAu alloy was studied in relation to aging time, degree of long-range order, and ordered domain size. The aging temperature of 200°C was chosen on the basis of the mechanical property studies of Nowack.[25] The kinetics of the process at this temperature are rapid enough to permit measurements within a practical length of time, yet slow enough to permit detailed study of the process. Hardness measurements provided an indication of the strength of the alloy. X-ray diffraction measurements on the bulk sample provided data which could be used for the determination of the LRO parameter and the ordered domain size corresponding to a given characteristic hardness.

X-ray Pattern Changes

Figures 6, 7, 8, and 9 show the change in the x-ray diffraction patterns for the CuAu sample disordered at 450°C and aged at 200°C for the accumulated times shown. Figure 6a presents the diffraction pattern for the sample in the as-quenched condition. Diffuse (001) and (110) superlattice humps can be distinguished even though no ordering treatment had been effected. After only two minutes aging (Figure 6b) these diffuse humps are seen to sharpen noticeably while the (200), (220), and (311) peaks begin to broaden at the base.

Figure 7a (six times accumulated aging time) show both the (001) and (110) superlattice peaks well resolved, with the (201) and (112)

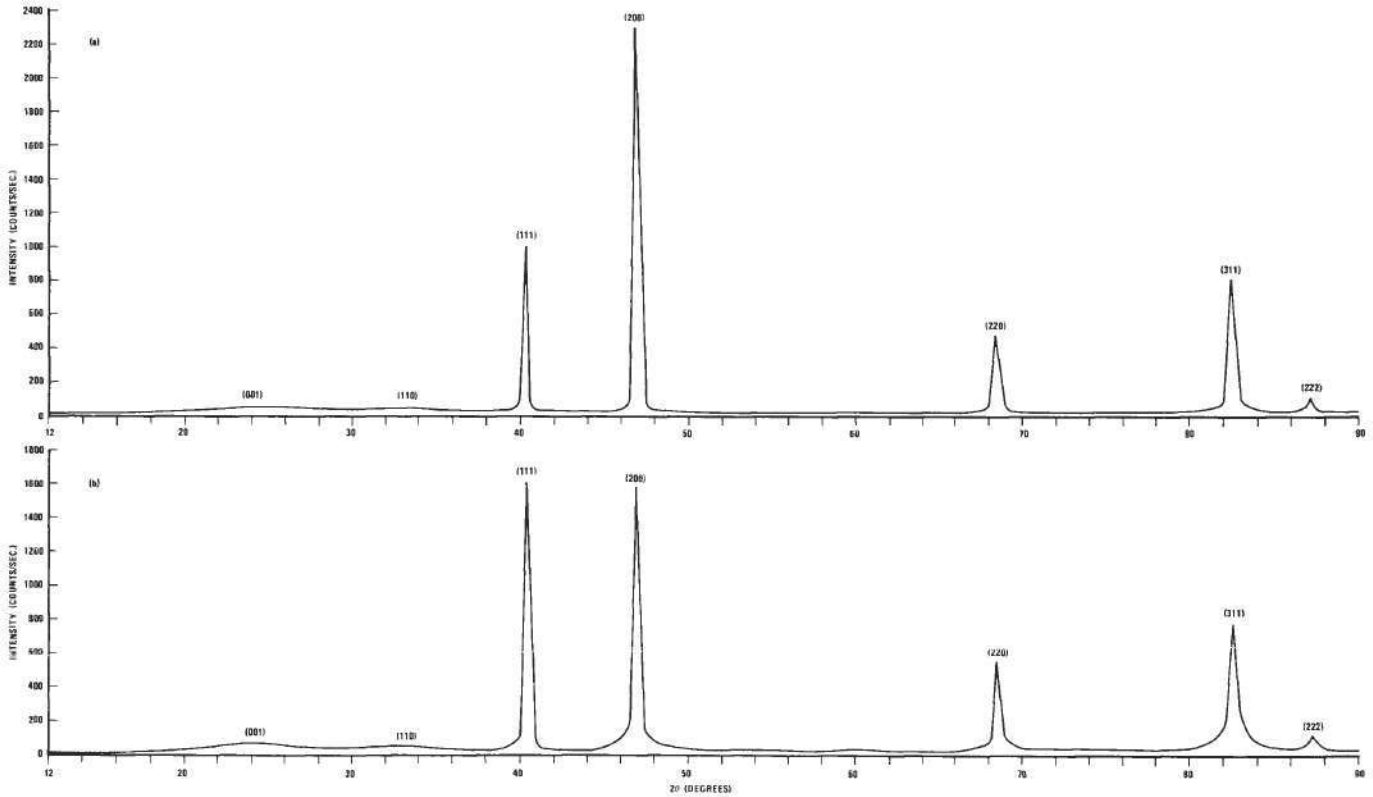

Figure 6. X-ray Diffraction Patterns for CuAu Disordered at 450°C: (a) As Quenched, (b) Aged Two Minutes at 200°C.

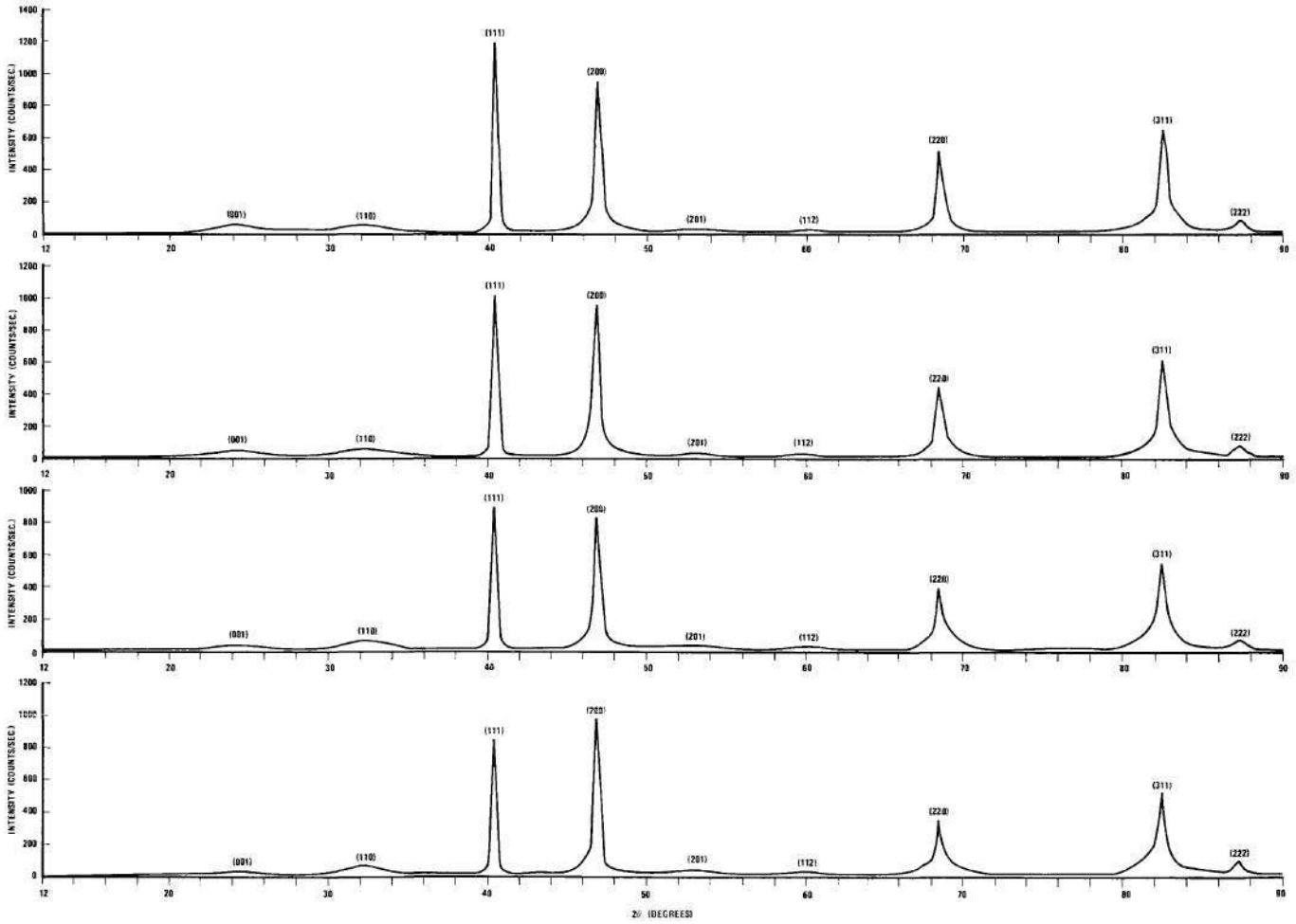

Figure 7. X-ray Diffraction Patterns for CuAu Disordered at 450°C then Aged at 200°C for: (a) Six Minutes, (b) Ten Minutes, (c) 18 Minutes, (d) 24 Minutes.

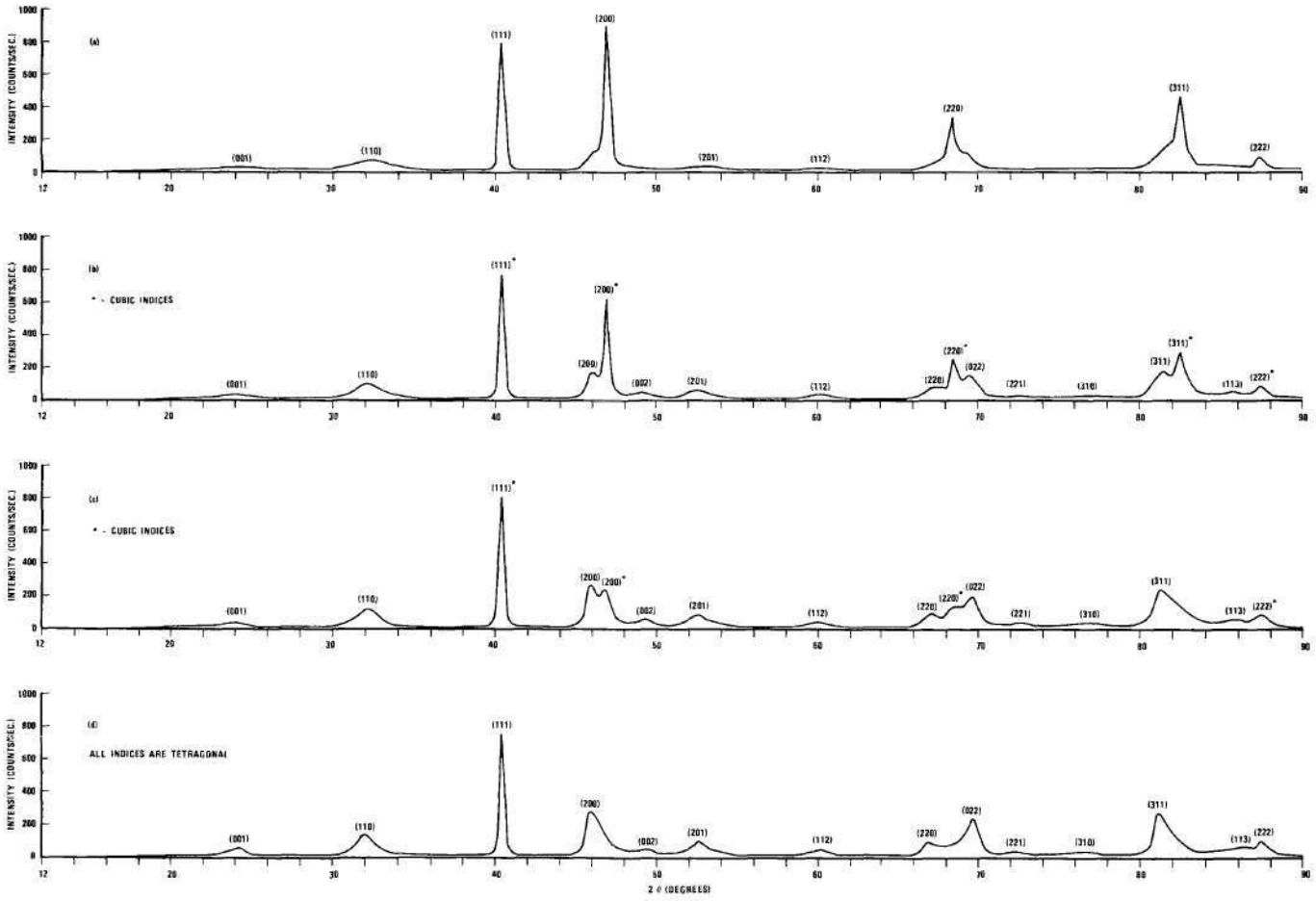

Figure 8. X-ray Diffraction Patterns for CuAu Disordered at 450°C then Aged at 200°C for: (a) 45 Minutes, (b) 180 Minutes, (c) 600 Minutes, (d) 1200 Minutes.

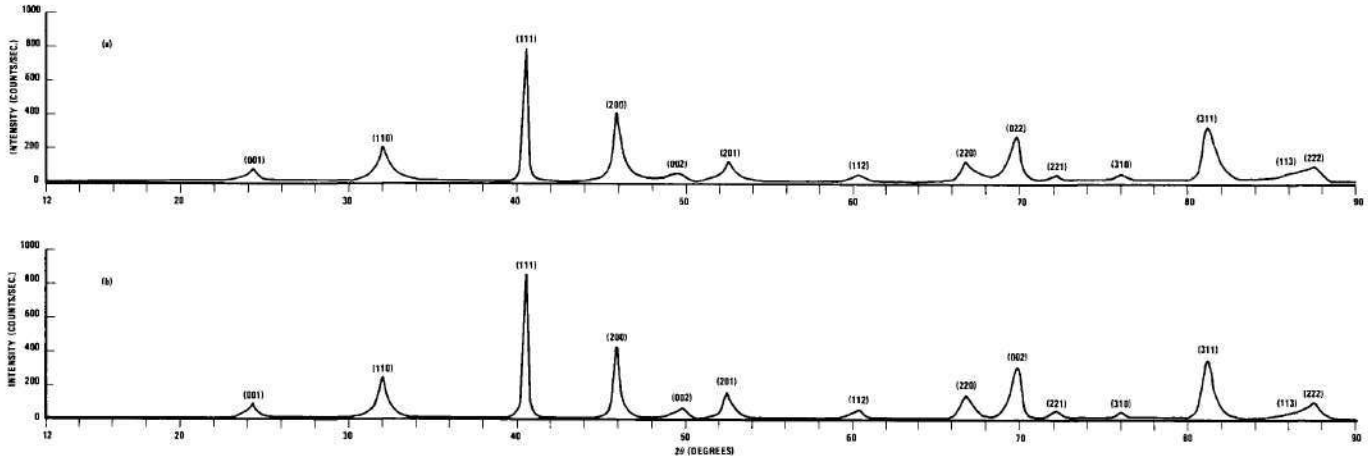

Figure 9. X-ray Diffraction Patterns for CuAu Disordered at 450°C then Aged at 200°C for: (a) 4200 Minutes, (b) 8400 Minutes.

superlattice peaks becoming distinguishable. Figures 7b through 8a show the decrease in intensity of the (001) peak, while the (200), (220), and (311) peaks continue to broaden. From Figures 8a, b, and c it can be seen that this broadening is due to the co-existence of the cubic and tetragonal peaks of the same indices. The intensity of the tetragonal peaks increases while that of the cubic peaks decreases. In Figure 8d the cubic peaks can no longer be distinguished.

In Figure 9 the tetragonal peaks are seen to sharpen as the influence of the cubic peaks continues to diminish. Figure 10 shows the diffraction pattern for the CuAu sample after disordering at 450°C and then aging at 350°C for six days. The Bragg-Williams LRO parameter corresponding to this treatment was 0.989, as calculated using the method of LeFevre and Starke.[33] The tetragonal peaks are all sharp and well resolved.

Hardness-Time Results

In Figure 11 the Vickers Pyramidal hardness number (VPN) of the CuAu sample is shown as a function of the logarithm of the accumulated aging time at 200°C. The hardness is seen to increase rapidly from an initial value of 170 to 257 within the first five minutes of aging, then decrease to a value of approximately 240 at 13 minutes aging. After about 18 minutes aging at 200°C the hardness jumps to 283 at about 23 minutes. The curve continues to increase at a decreasing rate until about 60 minutes aging has been completed. The increase is then approximately linear until the maximum of 330 is reached after about eight hours accumulated aging. The hardness then decreases rapidly,

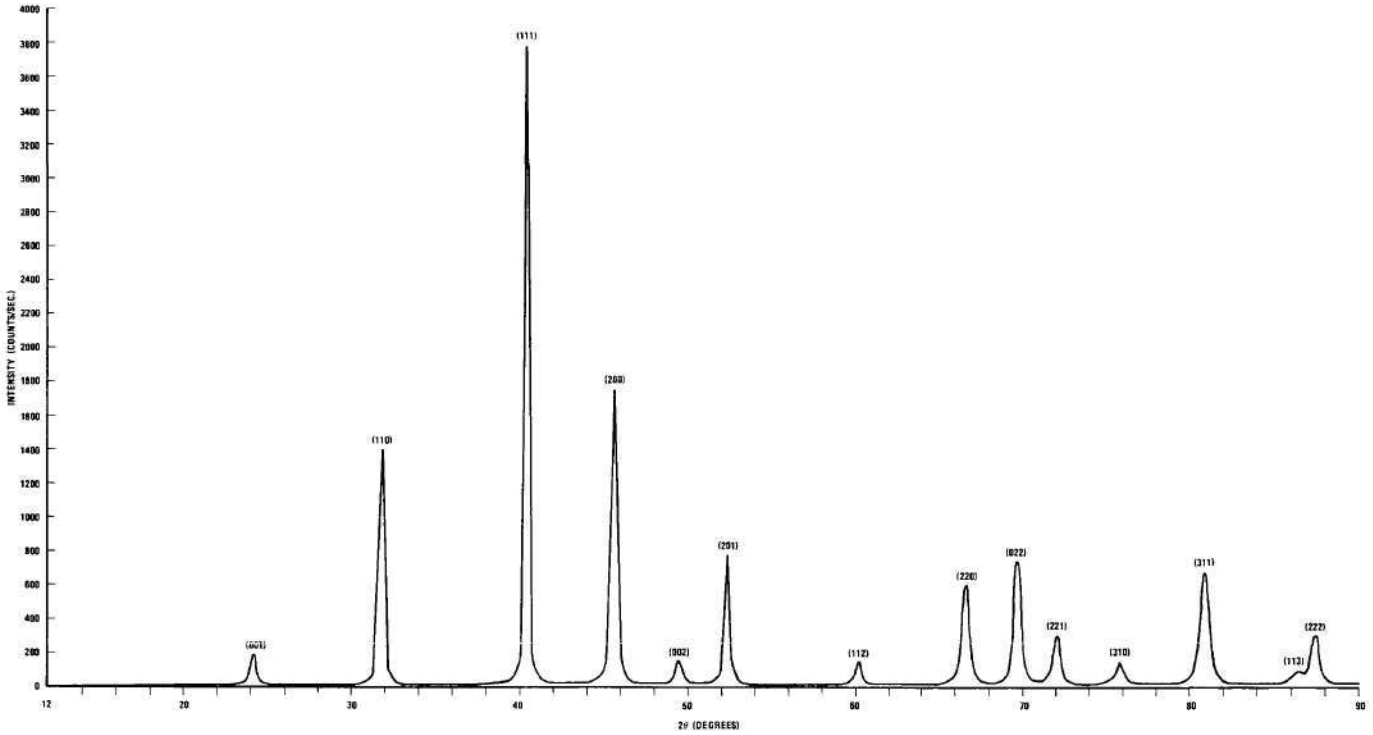

Figure 10. X-ray Diffraction Pattern for CuAu Disordered at 450°C then Aged for Six Days at 350°C.

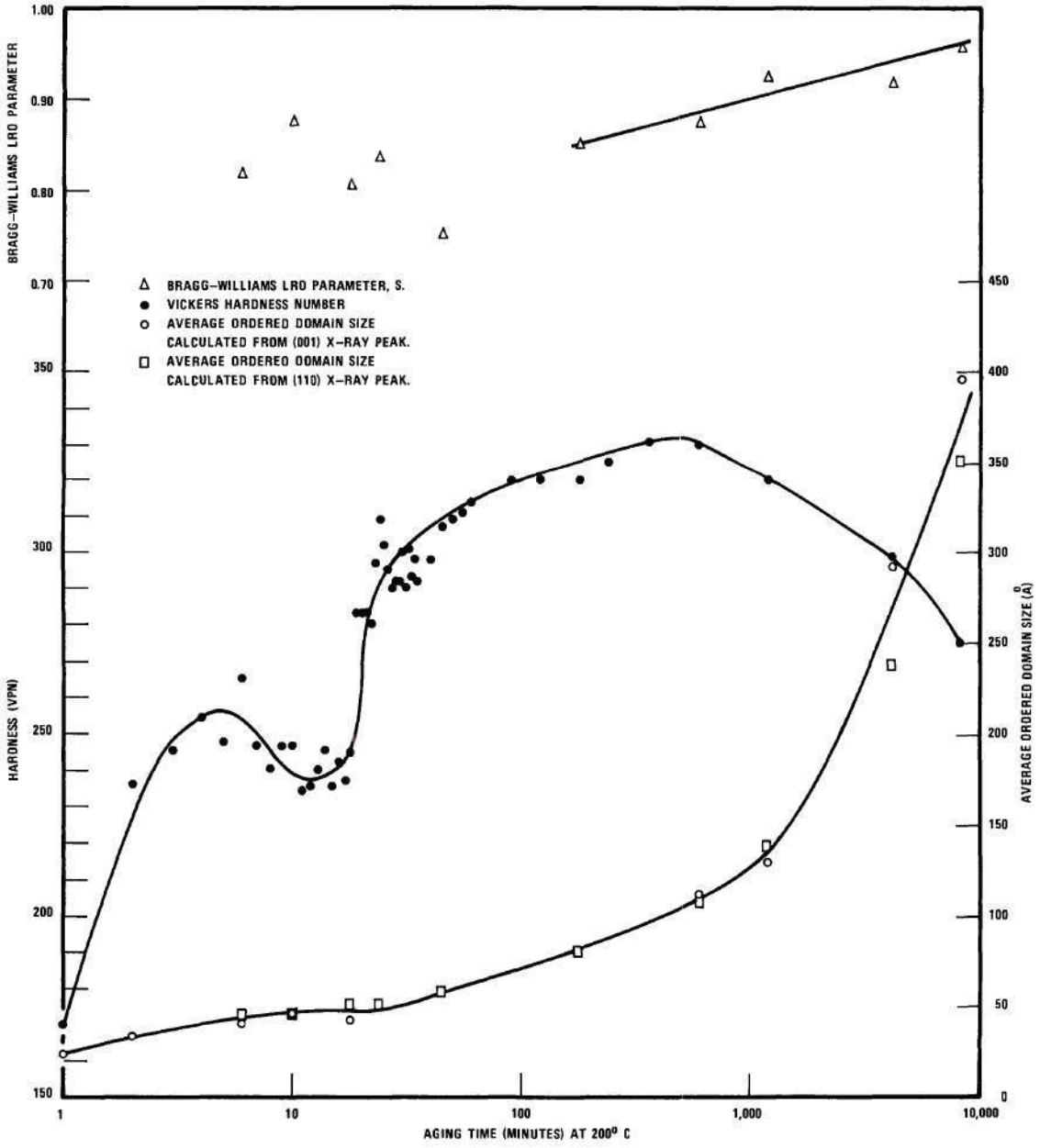

Figure 11. Bragg-Williams Long-Range-Order Parameter, Vickers Hardness Number, and Average Ordered Domain Size versus Aging Time at 200°C.

the final value obtained in the present study being 250 after 140 hours accumulated aging time.

Results Derived from X-ray Diffraction Data

Change in Breadth of the (111) Peak

Figure 12 shows the change in breadth of the (111) x-ray reflection at one half maximum intensity as a function of the logarithm of aging time at 200°C. This correlation was undertaken in order to determine whether or not any form of stress relief occurred in the region of the hardness drop seen in Figure 11.

Ordinarily it would be expected that the (111) peak would increase in breadth as internal strain within the sample increased. Any stress relief (e.g., by twinning) would cause the peak breadth to decrease, since part of the strain broadening would be removed. The situation is complicated in this alloy, however, by the fact that the observed (111) peak is in fact the sum of the $(111)_{cubic}$ and the $(111)_{tetragonal}$ peak. Thus it was necessary to investigate the rate of change in the (111) peak breadth.

It can be seen that the change in peak breadth increases continuously until approximately ten hours accumulated aging time, then drops off rapidly. No change in the rate of increase of the peak breadth is noted in the aging time interval from six to 20 minutes, the region of the dip in hardness.

Average Ordered Domain in Size

The average ordered domain size is plotted as a function of the logarithm of the accumulated aging time in Figure 11. The domain size

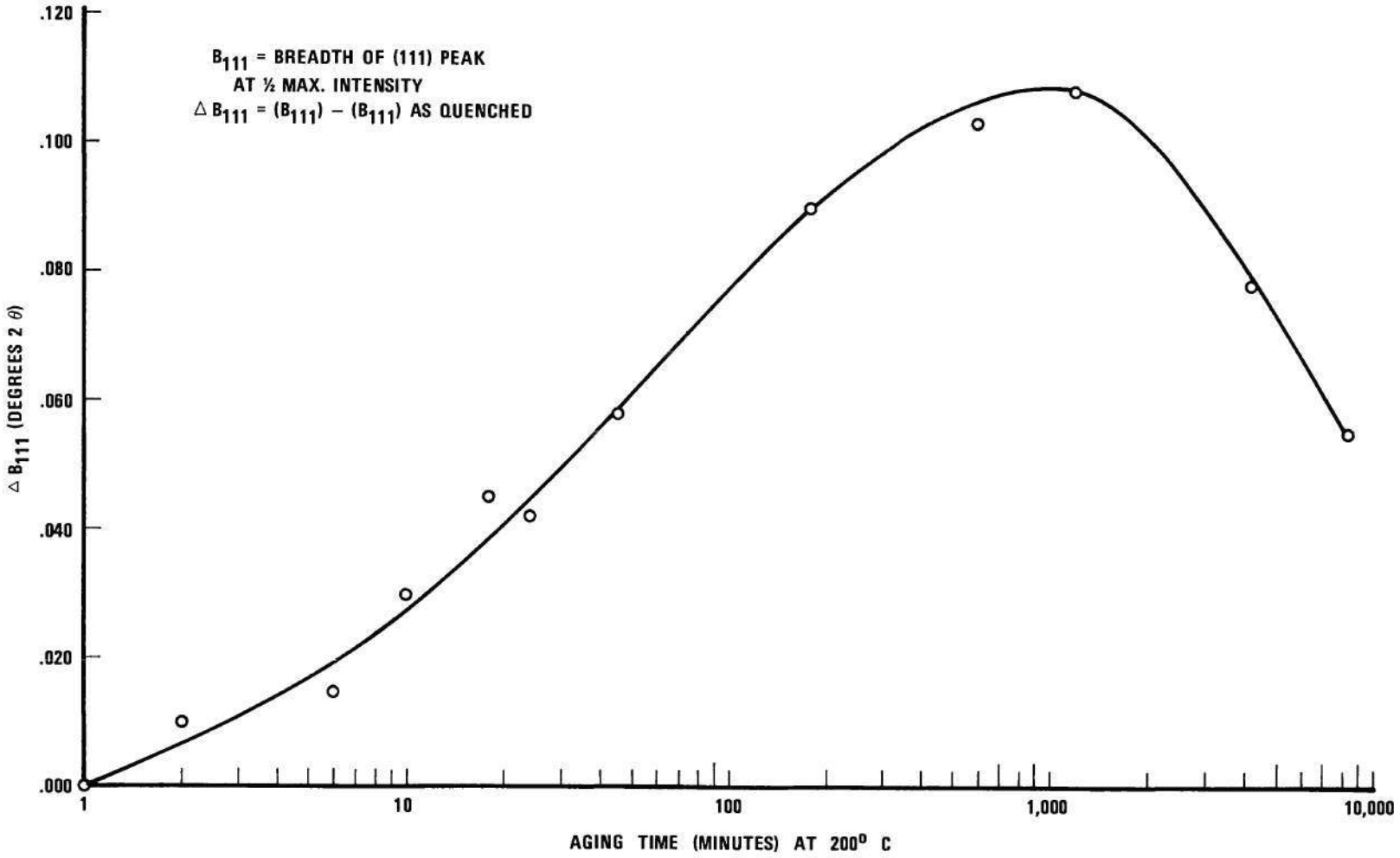

Figure 12. Rate of Change of (111) Peak Breadth with Aging Time.

increases slowly from a value of about 25 A in the as quenched condition to a value of about 45 A after ten minutes aging. No further change is observed until approximately 25 minutes aging is completed. The domain size increases more rapidly between 25 minutes and ten hours aging, where the rate of increase becomes very rapid. The maximum ordered domain size obtained in these measurements was approximately 375 A.

Bragg-Williams Long-Range-Order Parameter

As mentioned in Chapter II, the Bragg-Williams LRO parameter, S, was calculated in two ways. Figure 13 presents the LRO parameter calculated as in the work of Starke, Ogle, and Sparks[31] plotted as a function of the logarithm of the accumulated aging time. The value of S corresponding to an aging time of six minutes is 0.82. The values calculated from the (001) superlattice peak compared with the (200) fundamental peak, and from the (110) superlattice peak compared with the (220) fundamental peak are in very good agreement.

Figure 13 shows that the values of S calculated from these two peak pairs are in very poor agreement for accumulated aging times greater than six minutes. The average value of S appears to decrease from its original value of 0.82 at six minutes to a value of approximately 0.68 at 45 minutes. The LRO parameter then gradually increases to a value of about 0.80 after 140 hours aging. It can be seen that the divergence between the values of S calculated from the (001), (200) pair and the values calculated from the (110), (220) pair is as large as 40 per cent of the average value in some instances.

The Bragg-Williams parameter calculated by the method of LeFevre and Starke[33] is plotted in Figure 11 as a function of the logarithm of

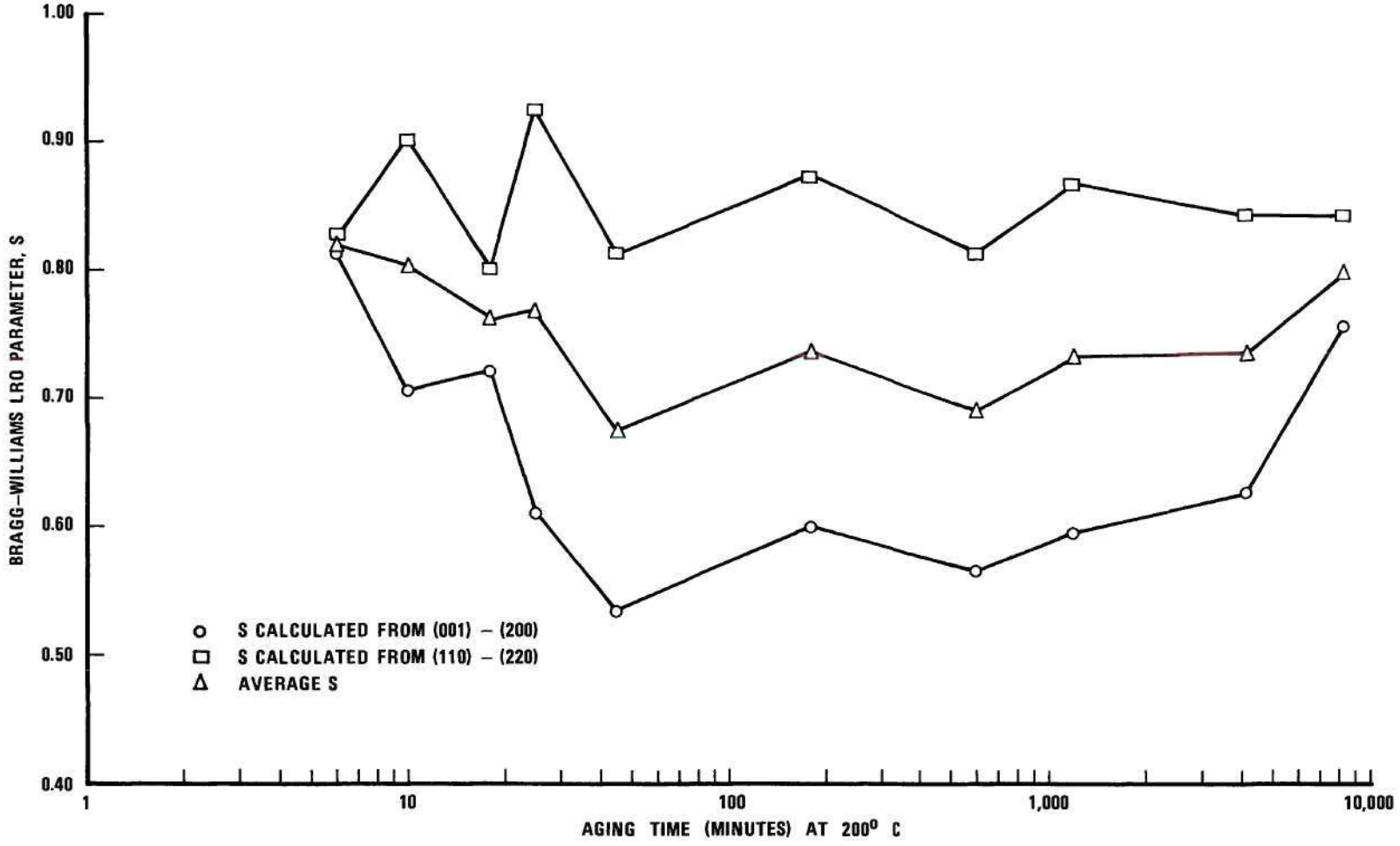

Figure 13. Bragg-Williams Long-Range-Order Parameter versus Aging Time at 200°C.

the aging time. The points calculated from x-ray data corresponding to accumulated aging times greater than 180 minutes seem to represent a continuously increasing curve. S increases from a value of 0.85 after 180 minutes aging to a value of 0.96 after 140 hours. Four superlattice peaks and five fundamental peaks were resolved and useable in the averaging procedure for each of these points.

In the case of the points corresponding to aging times less than 180 minutes, only two superlattice peaks could be resolved. It is felt that this is an insufficient number of peaks to warrant the assumption that the average of the texture coefficients for the superlattice peaks, $\left\langle T_i^0 \right\rangle$, is one. Therefore, no attempt was made to fit a curve to these points.

CHAPTER IV

DISCUSSION OF RESULTS

The most significant, and heretofore unreported, feature of the mechanical property measurements made in the present investigation is the transient decrease in hardness between five and 20 minutes accumulated aging time at 200°C. The use of the comparatively low aging temperature, and short aging time intervals permitted the detection of this feature.

Two possible explanations may be advanced to account for this hardness dip. Its existence might be correlated with theory of micro-twinning advanced by Hirabayashi and Weissman.[22] Arunachalam and Cahn[3] have questioned this theory partly on the basis of the lack of evidence of a drop in hardness values resulting from micro-twinning stress relief. The present results might seem to provide this evidence. Platerink[21] has reported a similar transient drop in shear modulus values for Cu_3Au on ordering. He explains this dip to be the result of the dissolution of ordered nuclei of sub-critical size. The observed hardness drop in the present measurements could be due to a similar reversion phenomenon.

As mentioned in Chapter III, the occurrence of twinning in the experimental sample would be expected to produce a decrease in the broadening rate of the (111) x-ray reflection. It was shown in Figure 12 that such an inflection is not seen in the region of the hardness dip. This conclusion is supported by the work of Hochman[35] who only observed twinning at much later stages of the aging process than our

observed hardness dip. It should be mentioned, however, that the controlling feature of the broadening is probably the co-existence of fcc and fct phases.

It is of interest to note that the average ordered domain size is constant in the region of the drop in hardness. After gradually increasing up to the time of the beginning of the hardness dip, the domain size becomes constant at about 45 A for its duration. As the hardness begins to increase, after about 20 minutes aging, the domain size once again begins to increase. The rate of growth is greater than the initial growth rate.

The behavior of the average size curve can be explained in terms of the reversion mechanism. Initially many small nuclei, which could have formed during the quenching operation, slowly grow. There is a critical nuclei size which must be obtained before rapid growth occurs. After approximately six minutes aging at 200°C, the sub-critical nuclei dissolve while the favored nuclei begin to grow at a more rapid rate. The two phenomena tend to cancel, and the result is an inflection in the domain growth curve. As the number of sub-critical nuclei decrease, the growth of the favored nuclei becomes the dominant effect. This results in an increased growth rate.

Figure 13 may be interpreted to imply a criterion for nucleus growth in addition to the critical size requirement. It was pointed out in Chapter III that the values of S calculated from the (001), (200) pair of x-ray peaks and from the (110), (220) pair are in good agreement for the six minute accumulated aging time. For longer aging times the agreement is quite poor. In fact, combined with the decrease in

intensity of the (001) superlattice peak seen in Figures 7b through 8a, implies that preferred orientation has become important, i.e., nuclei which possess certain orientation have preferred growth over others. Reasonable values of the Bragg-Williams parameter are obtained using the method of LeFevre and Starke[33] to remove the effect of texture, where enough peaks were resolved for the method to apply. It seems reasonable, therefore, to assume that the criteria for a given nucleus to be stable and grow are: (a) to attain a certain critical size and (b) to exist in a certain orientation. The ordering mechanism seems to involve random nucleation with a preferred growth orientation for continued growth.

In terms of the reversion mechanism, the hardness dip may be explained in the following way. The initial increase may be due to the formation and growth of many small ordered nuclei. Hardening results from the build-up of coherency strains, and from the interference to dislocation motion due to the presence of the nuclei, similar to the effect found in precipitation hardening alloys.

After approximately five minutes aging the nuclei which are sub-critical size, or which are unfavorably oriented, begin to dissolve. The reduction in interference to dislocation motion due to the reduction in the number of nuclei tends to reduce the hardening, while the increase in coherency strain associated with the growth of the favored nuclei tends to continue the hardness rise. While the nuclei dissolution is the dominant effect, the hardness decreases. When the dissolution of these nuclei nears completion, the increase in coherency strain becomes the most important factor. The hardness increases rapidly until the

maximum hardening associated with coherency strains for the existing stable nucleus size is attained. The hardness then increases at a rate consistent with the increase in coherency strain and tetragonal distortion strain associated with nucleus growth.

The hardening rate becomes fairly linear between one and five hours aging time. The hardness reaches its peak value of approximately 330 VPN after about eight hours aging. This behavior seems compatible with the build-up of coherency strain and tetragonal distortion strain. The rapid decay in hardness after ten hours aging results from relief of these strains. Mechanisms advanced to explain the stress relief include microtwinning to remove coherency strains[22] and twinning, recrystallization, and grain boundary migration.[3]

Reference to Figure 12 yields evidence for a rapid stress relief mechanism. It is seen that the (111) x-ray reflection begins to sharpen rapidly after about 20 hours aging. The fact that the peak breadth decreases more rapidly than it increased implies that the reduction in the contribution of the $(111)_{cubic}$ peak to the total intensity is not the only factor to be considered. A stress relief mechanism such as twinning or loss of coherency between the matrix and the ordered phase could contribute to the decrease in peak breadth.

It can be seen from Figure 11 that the average ordered domain size begins to increase rapidly at the same aging time as the (111) peak breadth begins to decrease. This implies that coherency between the ordered nuclei and the disordered matrix has been lost. The domains are free to grow faster due to the same effects which allow a high-angle grain boundaries to move more rapidly than low-angle boundaries in recrystallization.

CHAPTER V

CONCLUSIONS AND RECOMMENDATIONS

Conclusions

1. X-ray evidence and order parameter determinations indicate that ordering proceeds by random nucleation with growth of nuclei with a certain preferred orientation.

2. A transient drop in hardness exists at an early stage in the ordering of the alloy CuAu. This drop seems to be due to the dissolution of nuclei which have not attained a certain critical size or are not properly oriented.

3. An inflection in the growth rate of the ordered domains in the region of the hardness dip supports the proposal that dissolution of unfavored nuclei occurs.

4. The rapid increase in the growth rate of the ordered domains during the later stages of the ordering process results from the loss of coherency between the domains and the disordered matrix.

5. Due to the presence of preferred orientation during the early stages of ordering when only two superlattice peaks can be resolved, the Bragg-Williams LRO parameter, S, cannot be satisfactorily determined using a polycrystalline sample.

Recommendations for Future Studies

1. X-ray measurements using fine powders should be employed to determine the ordering behavior of CuAu during the early stages of the process.

2. Measurements similar to those of the present study should be undertaken in order to determine the effect of aging temperature on the transient hardness decrease.

3. A study should be initiated to determine the nature of the growth preferred orientation encountered in the present study.

APPENDIX

APPENDIX

SAMPLE CALCULATIONS

Average Ordered Domain Size Calculations

Calculation of B^*_{111}. From Chapter II it is seen that the equation for B^*_{111} is:

$$B^*_{111} = \frac{0.9\lambda}{t \cos \theta_S}$$

The value of t is obtained from:

$$t = \frac{0.9\lambda}{B_{111} \cos \theta_{111}}$$

For the CuAu sample aged for 1200 minutes at 200°C, B = 2.27×10^{-3} radians and $\theta_{111} = 20.18^\circ$. Therefore:

$$t = \frac{0.9(1.542 \text{ Å})}{(2.27 \times 10^{-3})(.9386)} = 652 \text{ Å}$$

The value of θ_S is 12.1°. Therefore:

$$B^*_{111} = \frac{0.9(1.542 \text{ Å})}{652 \text{ Å } (.9778)} = 3.08 \times 10^{-3} \text{ radians.}$$

Calculation of t_D. The equation for t_D, from Chapter II is:

$$t_D = \frac{0.9\lambda}{\sqrt{B^2 - (B^*_{111})^2} \cos \theta_S}$$

The value of B in this instance is 11.17 x 10^{-3} radians. Thus the value of t_D is:

$$t_D = \frac{0.9(1.542\ \text{Å})}{\sqrt{(11.17 \times 10^{-3})^2 - (3.08 \times 10^{-3})^2\ (.9778)}} = 130\ \text{Å}$$

Bragg-Williams Long-Range-Order Parameter Calculations

The value of S is calculated using the equation $S^2 = A/B$, where A and B are determined from equations (4) and (5) of Chapter II, respectively. The necessary values for the determination of S for the sample after 1200 minutes aging are found in Table 1. Thus the values of A and B are:

$$A = \frac{1}{I} \sum_{i=1}^{I} E_0^i/R_i^0 = \frac{0.0016 + 0.0046 + 0.0050 + 0.0035}{4} = 0.0037$$

$$B = \frac{1}{J} \sum_{j=1}^{J} E_j^f/R_j^f = \frac{0.0016 + 0.0045 + 0.0061 + 0.0059 + 0.0034}{5} = 0.0043$$

The values of S is then:

$$S = \sqrt{\frac{A}{B}} = \sqrt{\frac{0.0037}{0.0043}} = 0.928$$

Table 1. X-ray Data for CuAu Aged 1200 Minutes at 200°C

hkl	Type	2θ	θ	sinθ	sin2θ	$L = \frac{1}{\sin\theta\sin 2\theta}$	$\frac{\sin\theta}{\lambda}$	P	L.P.	$\frac{\sin^2\theta}{\lambda^2}$	$e^{-M_{Au}}$	$e^{-M_{Cu}}$	f_{Au}	f_{Cu}	F^2	M	R	E	
(001)	S	24.2	12.1	0.2096	0.4099	11.64	0.1359	0.942	10.96	0.0185	0.993	0.987	70.5	24.4	2109.6	2	46,242.4	72.97	0.0016
(110)	S	31.95	15.98	0.2753	0.5292	6.86	0.1785	0.906	6.22	0.0318	0.988	0.978	66.8	22.5	1935.1	4	48,145.3	220.58	0.0046
(111)	F	40.44	20.22	0.3456	0.6489	4.46	0.2241	0.860	3.84	0.0502	0.981	0.966	63.1	20.7	6707.6	8	206,057.5	325.8	0.0016
(200)	F	45.9	22.95	0.3899	0.7181	3.57	0.2529	0.829	2.96	0.0640	0.976	0.958	60.8	19.6	6102.7	4	72,256.0	456.8	0.0045
(002)	F	49.5	24.75	0.4187	0.7604	3.14	0.2715	0.809	2.54	0.0737	0.972	0.951	59.3	19.0	5732.0	2	29,118.6		
(201)	S	52.5	26.25	0.4423	0.7934	2.85	0.2868	0.791	2.25	0.0823	0.969	0.946	58.1	18.4	1512.4	8	27,223.2	135.56	0.0050
(112)	S	60.1	30.05	0.5008	0.8669	2.30	0.3248	0.749	1.72	0.1055	0.961	0.930	55.2	17.2	1372.7	8	18,888.4	66.72	0.0035
(220)	F	67.0	33.50	0.5519	0.9205	1.97	0.3579	0.718	1.41	0.1281	0.952	0.917	52.8	16.3	4253.6	4	23,990.3	406.95	0.0061
(022)	F	69.7	34.85	0.5714	0.9379	1.87	0.3706	0.706	1.32	0.1373	0.949	0.911	51.8	16.0	4062.8	8	42,903.2		
(311)	F	81.3	40.65	0.6501	0.9885	1.56	0.4216	0.674	1.05	0.1777	0.935	0.886	48.4	15.4	3458.0	16	58,262.4	443.95	0.0059
(113)	F	85.9	42.95	0.6814	0.9974	1.47	0.4419	0.668	0.98	0.1953	0.928	0.875	47.2	15.0	3241.0	8	25,409.4		
(222)	F	87.45	43.73	0.6913	0.9990	1.45	0.4483	0.666	0.97	0.2010	0.927	0.873	46.9	14.9	3191.1	8	24,762.9	83.20	0.0034

BIBLIOGRAPHY*

1. H. A. Bethe, Proc. Roy. Soc. A159, 1935, p. 552.

2. W. L. Bragg and E. J. Williams, Proc. Roy. Soc. A145, 1934, p. 699; A151, 1935, p. 540.

3. V. S. Arunchalam and R. W. Cahn, J. Mat'l. Sci. 2, 1967, p. 160.

4. J. C. Fisher, Acta Met. 2, 1954, p. 9.

5. R. W. Cahn, Local Atomic Arrangements Studied by X-ray Diffraction, Gordon and Breach, Chicago, 1965, p. 179.

6. M. J. Marcinkowski and D. S. Miller, Phil. Mag. 6, 1961, p. 871.

7. N. S. Stoloff and R. G. Davies, Acta Met. 12, 1964, p. 473.

8. P. C. Gehlen and J. B. Cohen, Phys. Rev. 139, 1965, p. 844.

9. P. A. Flinn, Trans. AIME 218, 1960, p. 145.

10. B. H. Kear, Acta Met. 12, 1964, p. 555.

11. R. G. Davies and N. S. Stoloff, Phil. Mag. 9, 1964, p. 349.

12. A. E. Vidoz and L. M. Brown, Phil. Mag. 7, 1962, p. 1167.

13. N. S. Krunakov, S. Zemczuzny, and M. Zasedatelev, J. Inst. Met. 15, 1916, p. 305.

14. C. H. Johansson and J. O. Linde, Ann. Physik 78, 1925, p. 439; 82, 1927, p. 449.

15. G. Borelius, J. Inst. Met. 74, 1948, p. 7.

16. D. Harker, Trans. ASM 32, 1944, p. 210.

17. G. C. Kuczynski, R. F. Hochman, and M. Doyama, J. Appl. Phys. 26, 1955, p. 871.

18. C. S. Barker, "Study of the Kinetics of Order-Disorder Transformations," Ph.D. Thesis, University of Notre Dame, 1954.

19. B. W. Roberts, Acta Met. 2, 1954, p. 597.

---

* Abbreviations found herein follow the form used by Nuclear Physics 1 (1956), p. 539, and 7 (1958), page 299.

20. K. Sato, D. Wanatabe, and S. Ogawa, J. Phys. Soc. of Japan 17, 1962, p. 1647.

21. G. R. Platerink, Phil. Mag. 17, 1968, p. 327.

22. M. Hirabayashi and S. Weissmann, Acta Met. 10, 1962, p. 25.

23. M. Hirabayashi and S. Ogawa, J. Phys. Soc. of Japan 11, 1956, p. 907.

24. J. L. O'Brien and G. C. Kuczynski, Acta Met. 7, 1959, p. 803.

25. L. Nowack, Z. Metallk. 22, 1930, p. 94.

26. N. S. Stoloff and R. G. Davies, The Mechanical Properties of Ordered Alloys - Progress in Materials Science, Pergamon Press, Vol. 13, 1966.

27. R. F. Fleischer, Acta Met. 8, 1964, p. 598.

28. R. G. Davies and N. S. Stoloff, Acta Met. 11, 1963, p. 1347.

29. C. J. Sparks and B. Borie, Local Atomic Arrangements Studied by X-ray Diffraction, Gordon and Breach, Chicago, 1965, p. 3.

30. B. D. Cullity, Elements of X-ray Diffraction, Addison-Wesley Publishing Co., Reading, Mass., 1959, p. 99.

31. E. A. Starke, Jr., J. C. Ogle, and C. J. Sparks, Jr., Advances in X-ray Analysis, Plenum Press, Vol. 12, 1969.

32. D. R. Chipman, J. Appl. Phys. 27, 1956, p. 739.

33. B. G. LeFevre and E. A. Starke, Jr., Advances in X-ray Analysis, Plenum Press, Vol. 12, 1969.

34. E. F. Sturcken, "An X-ray Method for Predicting the Stability of Natural Uranium at Low Burnups," U. S. Atomic Energy Commission Report DP-251, 1957.

35. R. F. Hochman, M. S. Thesis, University of Notre Dame, 1954.